INVESTIGATION OF BEAM ABERRATIONS AND BEAM HALO BY 3-DIMENSIONAL EMITTANCE MEASUREMENTS*

G.Riehl, J.Pozimski, W.Barth
Institut für Angewandte Physik der Johann Wolfgang Goethe Universität
Postfach 111932, D-6000 Frankfurt am Main, FRG

Abstract

We investigated the beam aberrations and beam halo caused by solenoids, Gabor lenses and Radio Frequency Quadrupoles. Thrfore we used a microprocessor controlled multifunctional profile- and emittance-measurement system. Online profile measurements, 2-dimensional slit-to-slit and also 3-dimensional point-to-slit emittance measurements have been made[1,2]. Construction of the measurement system and experimental results will be presented.

Concept of the Device

Fig. 1 shows a schematic diagram of the measuring device. Up to 4 slit/profile harp combinations may be installed to 6 stepping motor driven UHV feedthroughs. The profile currents of one harp are switched by a multiplexer to the 60-channel current amplifier. Motor and amplifier electronics are controlled by an 8-bit microprocessor system with digital I/O boards. This microprocessor is connected to a 68000-PC which handles interactive dialogs, data measurement, and data evaluation. The independent movable slits and profile harps provide online profile measurements, emittance measurements and also point-to-slit emittance measurements with crossed slits: The slits filter a beam partition of the coordinates x,y. The profile harps determine the angles x´ and y´ of this partition, therefore obtaining the beams charge distributions I(x,y,x´) and I(x,y,y´). Out of these 3-dimensional distributions calculation of all 2- and 1-dimensional subspaces of the beam distribution is possible[3,4].

Emittance Measurements behind a Solenoidal Lens

We used a plasma beam ion source[5] with a successive solenoidal lens[6] and extracted a 10 keV/3.6 mA He^+ beam. The ion beam occupies at least 75% of the lens aperture, causing aberrations of the beam phase space distribution. Fig.2 shows the measured x-emittance, the I(x,x´) distribution of the beam, measured with slit and profile harp. The convergent He^+ beam and a divergent neutral beam can be clearly distinguished. The dark 80% partition of the He^+ beam shows an 'S' shaped contour, due to the effect of the nonlinear solenoidal field. In addition, the phase space distribution has a 'butterfly' shape. The latter is caused by the radial symmetry of the nonlinear field, which twists different beam partitions I(x,x´,y) dependent on their position y. Fig. 3 shows the 2-dimensional beam profile, I(x,y) . We distinguish a high intense beam core, a homogenous middle part and increasing intensities at the edge of the

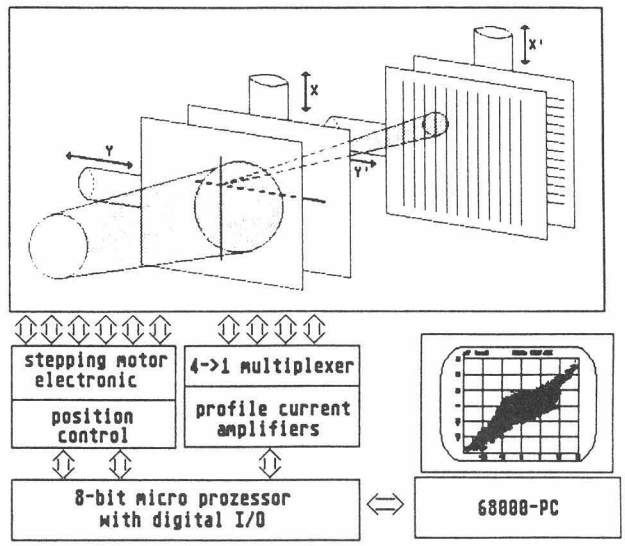

Fig.1: schematic drawing of the diagnostic device. Crossed slits and crossed profile harps provide measurements of the I(x,x´,y) and the I(y,y´,x) charge distributions

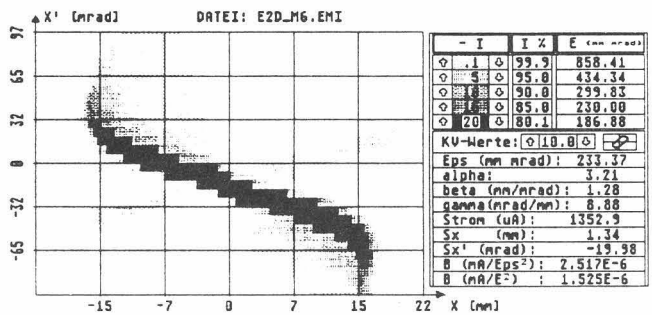

Fig.2: The distribution I(x,x´) of a 10 keV He^+ beam, measured with a slit/profile harp combination behind a solenoidal lens

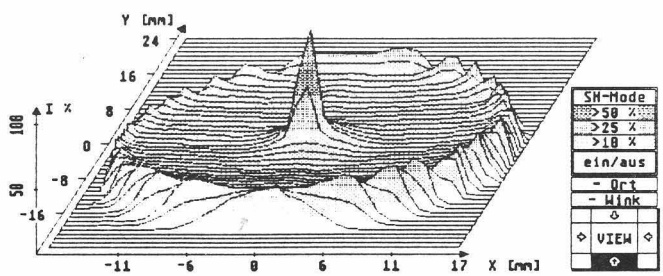

Fig:. 3: Distribution I(x,y) of the He^+ beam, calculated from the measured distribution I(x,x´,y)

beam. The distribution has a 'sombrero' like shape. The rim of this distribution is caused by strongly focused beam particles with shorter focal lengths than the inner part of the beam. Behind the beam focus these particles forms a wide halo. We measured the beam distribution I(x,x',y) with the point to slit method for the same beam parameters. Fig.4 shows different parts $I(x,x',y_i)$ of this measurement, with y=-14, -12, -10 and 0 mm. At the edge (y=-14mm) a small xx' distribution can be seen, showing less aberrations. The I(x,x',y=-12mm) distribution is characterized by an '8' shaped contour, which is caused by the nonlinear field in addition with the drift space inside the solenoid. The distributions next to the center of the beam show the same contour, but the '8' becomes wider. Therefore the 'butterfly' shape of the emittance and also the beam halo is composed out of different '8' shaped I(x,x',y) distributions. The marginal emittance is increased by the twisted 3-dimensional phase space distribution by a factor of 1.7 (90%) and 2.5 (99%). The RMS emittance is also affected by the 'S'-shaped filamentation, we calculate an RMS emittance growth of 1.5 (90%) and 2.2 (99%). Additional measurements with different beam and solenoid parameters and also computer simulations are in good agreement [7].

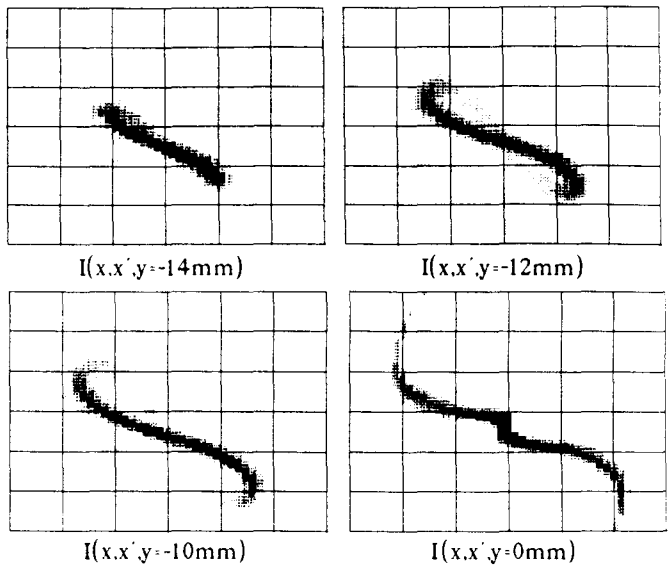

Fig. 4: He^+ beam distributions I(x,x',y) at different positions y, measured with two crossed slits and profile harp.

Emittance Measurements behind a Gabor Plasma Lens

For a second measurement series we replaced the solenoid by a Gabor plasma lens[8]. The figures show the phase space distributions of a 10 keV/ 125 µA Ar^+ beam behind the lens. Again the beam occupied a large fraction of the aperture. Fig . 5 shows the xx'- emittance of the beam measured with slit and profile harp, composed of an extreme high intense convergent 'butterfly', a second low intense convergent 'butterfly' and a divergent neutral beam. The 3-dimensional distributions I(x,x',y) (Fig .6) give an explanation of the structure of the 2-dimensional emittance: The Ar^+ beam is divided by the lens in a high intense central part and a low intense outer part, both showing the contour of an inverse 'S'. Compared with the shape obtained from solenoid measurements, the focusing strength inside the solenoid increases with radius, the Gabor lens shows a decreasing with radius. At the beam center decreasing charge intensities can be observed. The 2-dimensional beam profile in space (Fig. 7) shows, that we get a hollow beam. This may be explained by the incomplete filling of the lens by electrons occupying only the region near the axis.

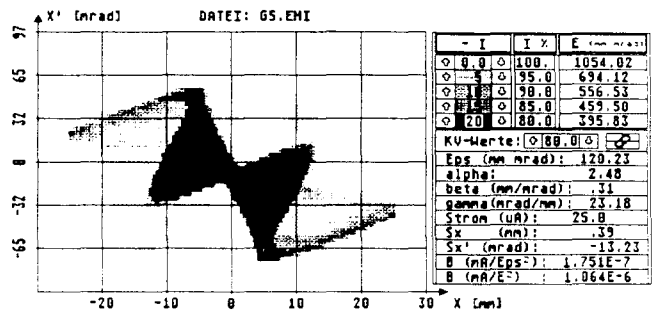

Fig.5 : Distribution I(x,x') of a 10 keV/125 µA Ar^+ beam, measured with slit and profile harp behind a Gabor plasma lens

Emittance Measurements behind a Split-Coaxial RFQ

For a third measurement series we connect ion source, solenoid and a split-coaxial RFQ[9]. The figures show the phase space distributions of a 50 keV/ 800 µA He^+ beam behind the accelerator. The perspective view to the beam emittance (Fig. 8) shows elliptical contours without any remarkable twist or filamentation. The 3-dimensional distributions $I(x,x',y_i)$ (Fig.9) show a filamentation of the ion beam and in all distributions two

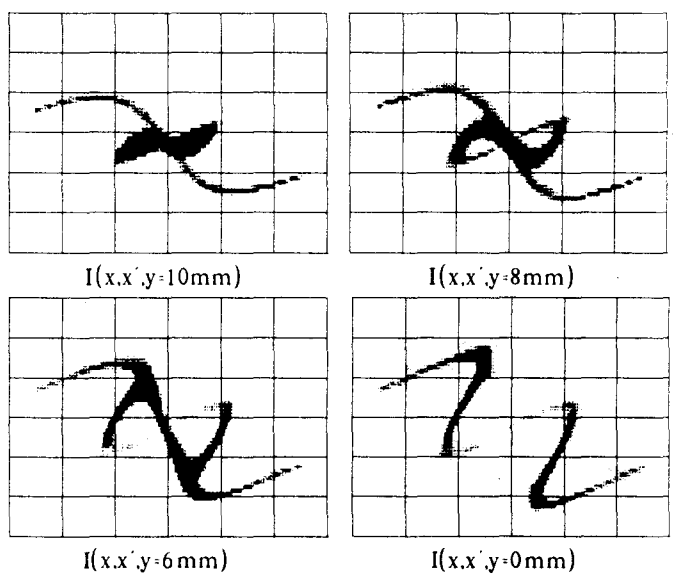

Fig.6: 3-dimensional distributions of the Ar^+ ion beam

beam centers can be clearly distinguished. The ion beam separates into two parts. This leads to an emittance growth of 1.4 (90%). The beam profile in space (Fig.10) shows a rectangle, nearly homogenous charge distribution.

Conclusion

The diagnostic device is a powerful tool to investigate 1-, 2- and 3-dimensional phase space distributions of ion beams. The analysis of the 3-dimensional distribution I(x,x',y) and I(y,y',x) gives important information about the genesis of beam halo, emittance aberrations and emittance growth. All experimental results show filamentation of the phase space distribution of the beam which increases the beam emittance. Further development of the device will include reconstruction of the 4-dimensional phase space distribution I(x,x',y,y').

*work supported by the BMFT under contract number 06 OF1861

Reference

1 T.Weis et. al. "Emittance growth... ", this conference
2 A.Schempp, "The CRYRING RFQ", EPAC-90, Nice
3 G.Riehl, Internal Report 89-14, Institut für Angewandte Physik D-6000 Frankfurt/M. , Pstf. 111932, FRG
4 G.Riehl, Internal Report 89-16 , mailing adress see [3]
5 K.Langbein, IEEE Catalog No. 87CH2387-9 1987, Vol.1, p.379
6 A. Müller-Rentz, diploma thesis 1985, mail. adr. see [3]
7 G. Riehl, J. Pozimski, W. Barth, Interner Report 90-14, mailing adress see [3]
8 J. Pozimski, diploma thesis 1990, mail. adr. see [3]
9 P.Leipe, diploma thesis 1985, mail. adr. see [3]

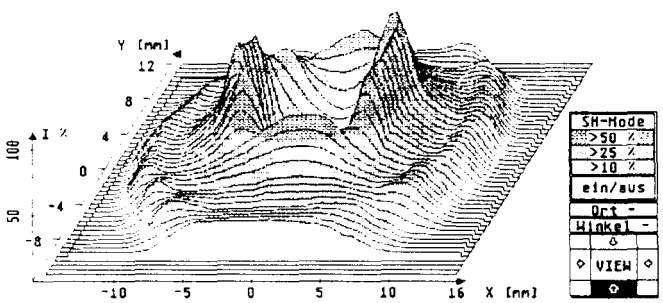

Fig. 7 : perspective view to the Ar^+ beam distribution I(x,y)

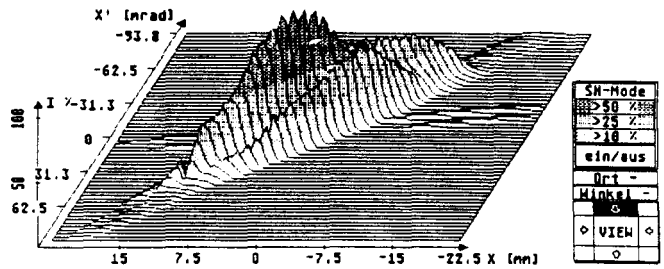

Fig. 8: perspective view to the He^+ beam emittance behind the split-coaxial RFQ

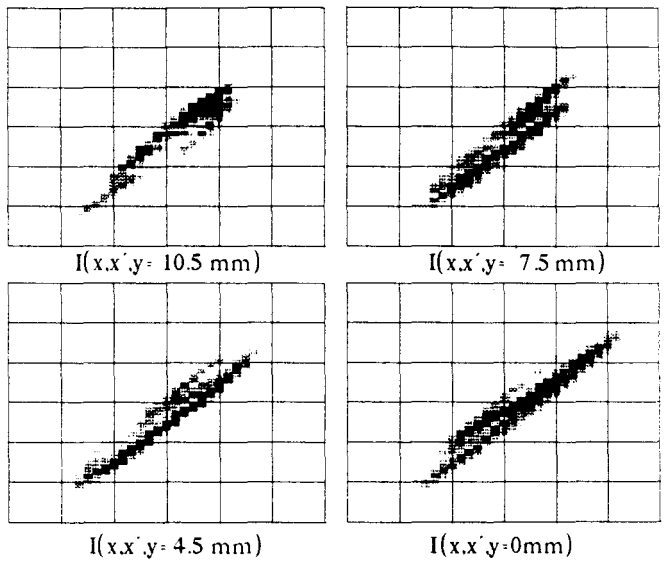

Fig. 9: He^+ beam distributions I(x,x',y) at different positions y.

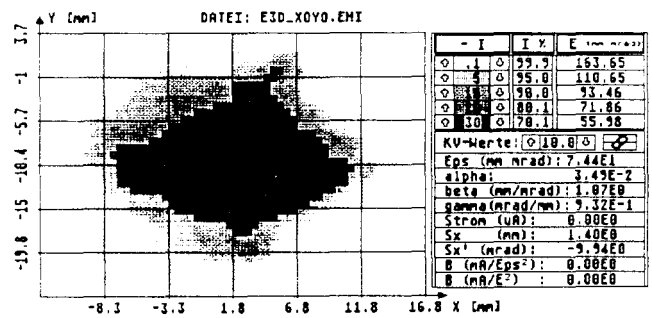

Fig. 10: The He^+ beam profile I(x,y)